Journal of Photochemistry and Photobiology A: Chemistry 225 (2011) 81–87

Contents lists available at SciVerse ScienceDirect

Journal of Photochemistry and Photobiology A: Chemistry

journal homepage: www.elsevier.com/locate/jphotochem

Phosphorus-doped titania nanotubes with enhanced photocatalytic activity

Ramesh Asapu, V. Manohar Palla, Bin Wang, Zhanhu Guo, Rakesh Sadu, Daniel H. Chen*

Photocatalysis and Solar Processing Lab, Dan. F. Smith Department of Chemical Engineering, Lamar University, Beaumont, TX 77710, USA

ARTICLE INFO

Article history:
Received 12 August 2010
Received in revised form 20 August 2011
Accepted 3 October 2011
Available online 8 October 2011

Keywords:
Nanotubes
Titania
Photocatalysis
Phosphorus doping
Band gap
Rhodamine B

ABSTRACT

Titania nanostructures have gained much attention lately due to their high specific surface area, ion-exchange ability, and better electrical properties. In this study, pure titania nanotubes (TNTs) were synthesized using hydrothermal method. Phosphorus-doped titania nanotubes (P-TNTs) were fabricated following a wet chemical procedure with dimethyl phosphite as a precursor. Characterization of the prepared pure/phosphorus-doped titania nanotubes was performed using transmission electron microscopy (TEM), energy dispersive X-ray spectroscopy (EDX), XRD analysis, UV–Vis absorption spectra, and BET specific surface area analysis. Phosphorus-doping slightly reduces the surface area but shifts the band gap towards the visible light region. When compared to pure TNTs, the optimal 0.75 wt.% P-TNTs have a similar surface area (272 m^2/g vs. 274 m^2/g) but with a band gap shift of 0.27 eV towards the visible light region. The photocatalytic activity of 0.75 wt.% P-TNTs was tested using rhodamine B (RhB) as a model pollutant under a 9 W fluorescent lamp and was significantly better than the benchmark Degussa P25 nanoparticles due to the band gap narrowing and an increased surface area. The decolorization follows first-order kinetics with the apparent rate constant k_1 of 0.13 min^{-1} for 0.75 wt.% P-TNT and 0.07 min^{-1} for Degussa P25.

1. Introduction

Titanium oxide or titania has been used widely in photovoltaic solar cells, water-splitting catalysts for hydrogen generation, and in gas and liquid phase pollution control such as photocatalytic oxidation of volatile organic compounds (VOCs) and NO_x [1–4]. In most of the catalytic applications, high surface area and optimum pore size are needed for interaction with active sites and diffusion of reactive species [5], this leads to the development of titania based nanotubes, nanowires, and nanorods. In photocatalysis, the electron–hole recombination step results in waste of energy supplied by the photon and can be considered as one of the major factors limiting the efficiency of photocatalytic processes. Some researchers have suggested that recombination effect is greatly reduced in nanotubes architecture compared to nanopowders and should be favored in photocatalytic applications [6]. Also, the high specific surface area, ion-exchange ability, and better electrical properties have given titania nanotubes a superior platform. Titania nanotubes are used extensively in the research of hydrogen production, fuel cell applications, and photocatalytic applications [6,7]. A suitable method to enhance the photocatalytic ability of titania nanotubes is post treatment of titania nanotubes including introduction of impurities (or doping) to increase the visible light responsiveness. Pure titania nanotubes doped with different metals like Cu, Zn, Cr, and Fe [8–11] and non metals including N, S, C, and F [12–14] have been reported. In fact, doping of titania nanotubes is a subject of broad interest for the past few years. To our knowledge preparation of phosphorus-doped titania nanotubes using simple wet chemical method has not been reported.

Titania based nanotubes can be synthesized using different methods such as electrochemical anodic oxidation, also known as anodization [15,16], template-assisted methods [17,18], and hydrothermal method [19,20]. Each fabrication method has its own distinctive advantages and functional features. Hydrothermal method is of particular interest because nanotubes can be produced in an unsophisticated manner at low temperatures and through simple wet chemical synthesis routes. In this paper, pure titania nanotubes were synthesized using the hydrothermal method, and a simple wet chemical procedure was used to dope phosphorus into the nanotubes. Phosphorus-doped titania nanotubes were prepared by treating titania nanotubes in aqueous solution of dimethyl phosphite followed by calcination at high temperatures.

2. Experimental methods

2.1. Reagents and materials

Titanium dioxide (Degussa P25) was obtained from Evonik Industries and sodium hydroxide (NaOH 10 N) was obtained from Lamar Ka, Inc. Hydrochloric acid (HCl 1 M), dimethyl phosphite

* Corresponding author. Tel.: +1 409 880 8786; fax: +1 409 880 2197.
E-mail address: daniel.chen@lamar.edu (D.H. Chen).

1010-6030/$ – see front matter © 2011 Elsevier B.V. All rights reserved.
doi:10.1016/j.jphotochem.2011.10.001

(DMP $C_2H_7O_3P$, 99.8 wt.%), ethanol (200 proof), and rhodamine B (RhB) were purchased from Sigma Aldrich. All chemicals were of analytical grade and used without further purification, and all the water used was deionized.

2.2. Synthesis of titania nanotubes

Titania nanotubes were synthesized following a literature procedure [19,20]. About 5 g of pure TiO_2 (Degussa P25) powder was dispersed in 175 ml of NaOH (10 N) solution, and the suspension was transferred into a Teflon-lined stainless steel autoclave (Parr Inst.) and sealed. The autoclave was maintained at a temperature of 130 °C for 24 h and then allowed to cool to room temperatures. The white precipitate obtained from the hydrothermal treatment was vacuum-filtered and washed with 0.1 N HCl and deionized water until the pH was around 7. The sample was then dried at 100 °C overnight to obtain titania nanotubes denoted as TNTs.

2.3. Synthesis of phosphorus doped titania nanotubes

Phosphorus-doped titania nanotubes were fabricated using a facile wet chemical method. The analytical grade pure dimethyl phosphite was diluted to known concentrations using ethanol. TNTs (1 g) were dispersed in this ethanol solution of dimethyl phosphite through sonication. The mixture was magnetically stirred overnight followed by drying at 80 °C for 4 h. Finally, the product was calcined at 350 °C in a muffle furnace for 1 h with a heating rate of 1 °C/min. These phosphorus-doped titania nanotubes are denoted as P-TNTs.

3. Characterization

The morphology of the samples was observed using a Philips CM-200 transmission electron microscope (TEM) with a LaB6 filament operated at an accelerating voltage of 200 kV. A HITACHI S-3400 N scanning electron microscope (SEM) attached with energy dispersive X-ray spectrometry (EDX) was used to determine the elemental composition. X-ray diffraction (XRD) analysis was performed on a Bruker D8 Focus diffractometer equipped with a Sol-X detector using a copper radiation source. Specific surface area analysis was done using the Brunauer, Emmett, and Teller (BET) method based on N_2 adsorption at 77 K with a NOVA 1000 series analyzer. The UV–Vis absorption spectra of samples were recorded using a UV–Vis double beam spectrophotometer (Cary 100, Varian Inc.) attached to an internal diffuse reflectance accessory.

4. Results and discussions

4.1. TEM observation

TEM images provide an understanding into the nanostructure morphology of the samples. From the TEM images (Figs. 1 and 2), we clearly see that the nanotubes are uniform and open ended. The nanotubes are approximately 100–200 nm long with an outer diameter 12 nm and inner diameter of 6 nm. After phosphorus doping, titania nanotubes retain the tubular structure as observed from Fig. 2. It was also observed that when the calcination temperature was raised from 350 °C to 500 °C, the nanotubes started to break apart, fuse together, and form lumps of nanoparticles and/or nanorods (data not shown).

4.2. X-ray diffraction analysis

To identify the crystal phase of the nanotubes, X-ray diffraction analysis was done. From the X-ray diffraction patterns, it was observed that pure titania nanotubes have peaks which can be mostly assigned to anatase phase similar to those of Degussa P25 (Fig. 3). The peaks at 11° can be attributed to a hydrogen titanate phase ($H_2Ti_3O_7$), which is a monoclinic unit cell structure [21]. The diffraction patterns of pure and phosphorus-doped titania nanotubes (both calcined at 350 °C) show some increase in the intensity of anatase peaks and diminishing of the hydrogen titanate peak compared to uncalcined pure titania nanotubes.

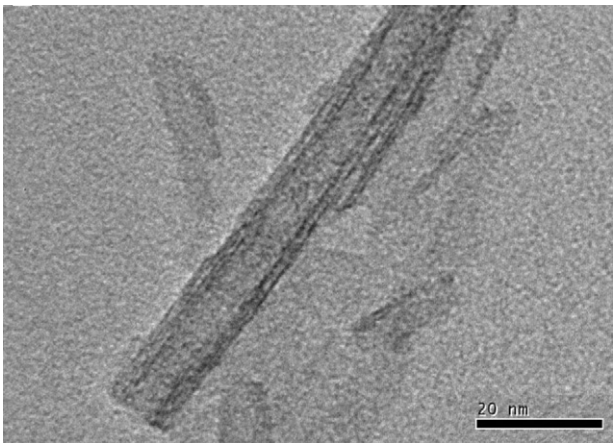

Fig. 1. Magnified TEM image of titania nanotube.

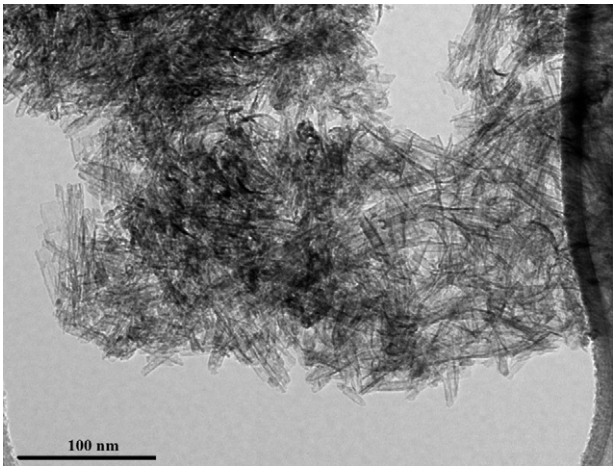

Fig. 2. TEM image of phosphorus-doped titania nanotubes.

4.3. Brunauer–Emmett–Teller surface area analysis

Specific surface area of the nanotubes samples were determined using the Brunauer, Emmett, and Teller (BET) method based on N_2 adsorption/desorption isotherm at 77 K. The specific surface area values are shown in Table 1. There is a significant decrease in the BET surface area due to calcination and phosphorus-doping,

Table 1
Specific surface area of photocatalyst samples using BET method.

Sample	Specific surface area (m^2/g)
Degussa P25	50
Titania nanotubes	306
Titania nanotubes calcined at 350 °C	274
0.75 wt.% phosphorus-doped titania nanotubes	272
12 wt.% phosphorus-doped titania nanotubes	136

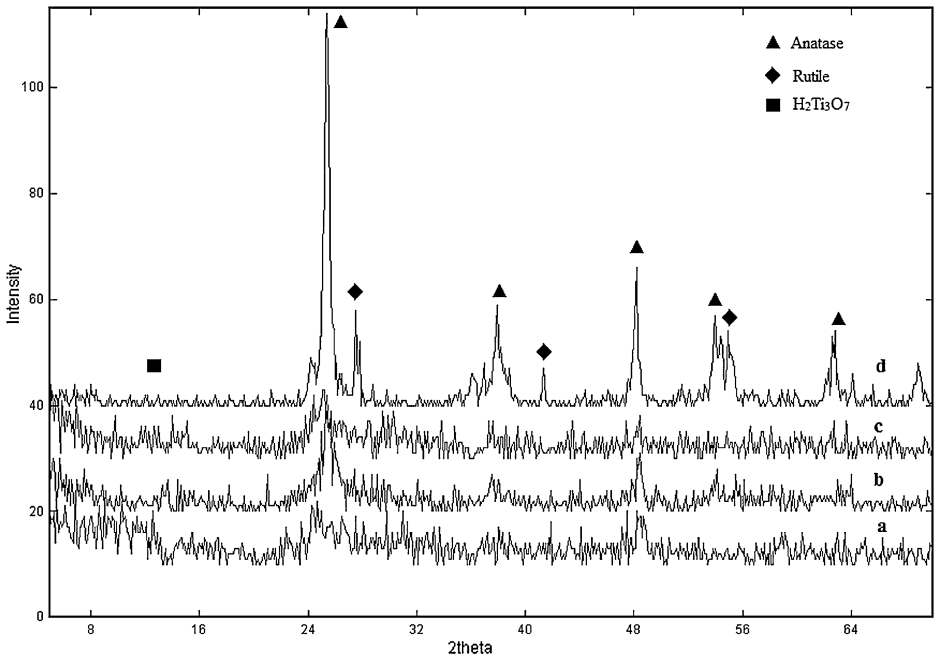

Fig. 3. X-ray diffraction patterns of (a) titania nanotubes, (b) titania nanotubes calcined at 350 °C, (c) phosphorus-doped titania nanotubes, and (d) Degussa P25.

which includes a calcination step. Further, as the phosphorus content increases, there is a substantial decline in the availability of surface area for photoreaction.

4.4. UV–Vis absorption spectrum

The optical properties of the photocatalyst materials were studied with the help of UV–Vis spectrophotometer. The band gaps of these samples were estimated from plots of the modified Kubelka–Munk function vs. the energy of exciting light [22]. From Fig. 4, we can approximate the band gap energies of Degussa P25 TiO_2 nanoparticles and as-prepared TNTs to be 3.06 eV and 3.22 eV, respectively. The band gap value of commercial Degussa P25 is found to vary between 3 and 3.2 eV in the literature [23,24]. After calcination, the band gap of pure titania nanotubes changes from 3.22 eV to 3.14 eV. P-TNTs have a band gap energy of 2.95 eV, which corresponds to light energy in the visible region (420 nm). Thus the phosphorus doping on TNT induces a shift of the absorption edge slightly towards the visible light range (from 385 nm to 420 nm) and the narrowing of band gap by 0.27 eV (shift from 3.22 to 2.95 eV). This result is supported by slight color change from white to light yellow after phosphorus doping.

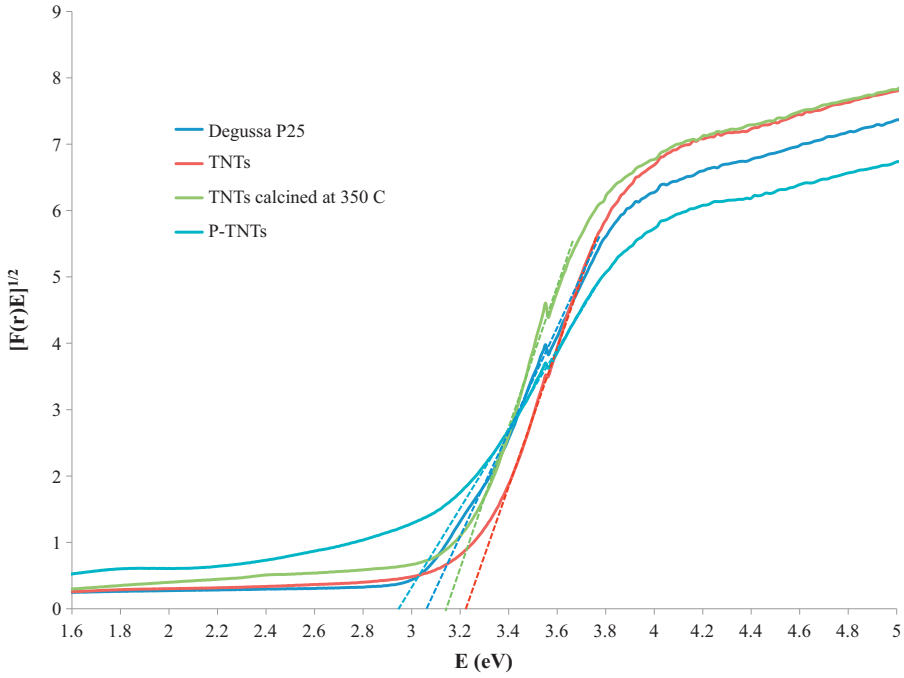

Fig. 4. Plot of the transformed Kubelka–Munk function vs. photon energy.

4.5. EDX analysis

Energy dispersive X-ray spectroscopy (EDX) analysis of the samples reveals the presence of Ti and O as elements (except for H, as it cannot be detected in EDX) in titania nanotubes. From EDX analysis, the atomic ratio of Ti:O is 3:7, which proves the XRD analysis supporting the assumption of $H_2Ti_3O_7$ monoclinic unit cell structure. Phosphorus was also detected, in addition to Ti and O, in phosphorus-doped titania nanotubes. The weight percentage of phosphorus was found by averaging the values from two different analyses of the same sample to adjust the error in detection. Average weight percentage contents of phosphorus detected by EDX are: 12 wt.%, 6 wt.%, 1.5 wt.%, 0.75 wt.%, and 0.5 wt.%. To obtain a nominal 12 wt.% and 0.75 wt.% of phosphorus content, 2% and 0.05% dimethyl phosphite solutions were used as precursors respectively.

4.6. Effect of hydrothermal synthesis temperature on morphology

The hydrothermal synthesis temperature or the temperature at which TiO_2–NaOH suspension is autoclaved plays a significant role in the morphology of the resulting nanotubes. To investigate the effect of hydrothermal synthesis temperature, a specific batch was synthesized at 180 °C. The post treatment process of washing with acid and de-ionized water was the same for this batch. The resultant nanotubes were analyzed with TEM to determine diameter and length. As observed from the TEM image (Fig. 5), nanotubes synthesized at 180 °C are not uniform in size, but rather a mixture of nanotubes and nanorods. These nanotubes have an outer diameter in the range of 25 to 100 nm and are 400 nm to 4 μm long. The BET surface area of this batch is 100 m^2/g, far less when compared to nanotubes synthesized at 130 °C (BET surface area 306 m^2/g). This is due to the destruction of the tubular structure and the formation of large nanorods when the hydrothermal synthesis temperature was increased to 180 °C.

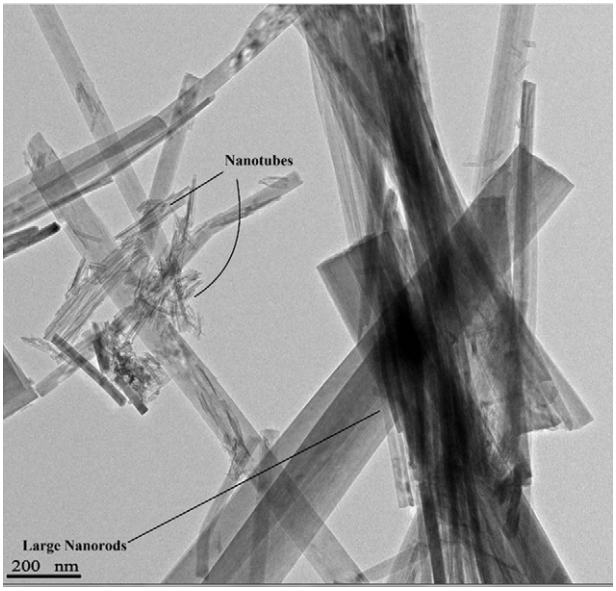

Fig. 5. TEM image of titania nanostructures synthesized at 180 °C consisting of nanotubes and nanorods.

5. Photocatalytic activity

The photocatalytic activities of the titania nanotubes were examined by conducting experiments in a 250 ml glass reactor vessel. The reactor was wrapped with aluminum foil and the reaction mixture was irradiated with a 9 W fluorescent lamp (Philips PL-S 9 W). Around 0.45 g of photocatalyst was added to 150 ml of RhB solution (2 mg/l). The contents were stirred magnetically during the irradiation period. An experiment was run for 2 h to observe any degradation of RhB exposed to the light source in the absence of catalyst. There was no degradation at all under the fluorescent lamp. The reaction mixture was stirred in dark to reach adsorption equilibrium before the light source was turned on. Samples were withdrawn and analyzed with the CARY 50 UV–Vis spectrophotometer at 554 nm to measure the absorbance of the sample. From the Beer–Lambert law $A = \varepsilon lc$, where ε represents molar absorption coefficient, l is path length, and c represents a concentration of sample. Since the path length and absorption coefficient of RhB are constant, we can relate absorbance directly to concentration. To have a comprehensive comparison among the photocatalyst materials prepared, the reaction conditions are kept the same for all the activity tests.

As shown in Fig. 6, P-doped TNT with 0.75 wt.% phosphorus content has the best activity and pure TNT also exhibits a good activity.

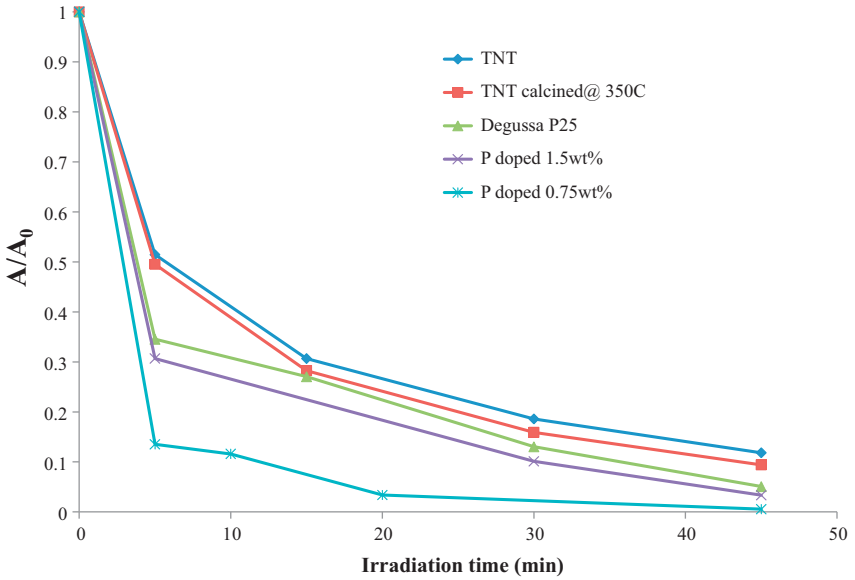

Fig. 6. Photocatalytic degradation of rhodamine B under the irradiation of a 9 W fluorescent lamp (best photocatalyst: 0.75 wt.% P-TNT).

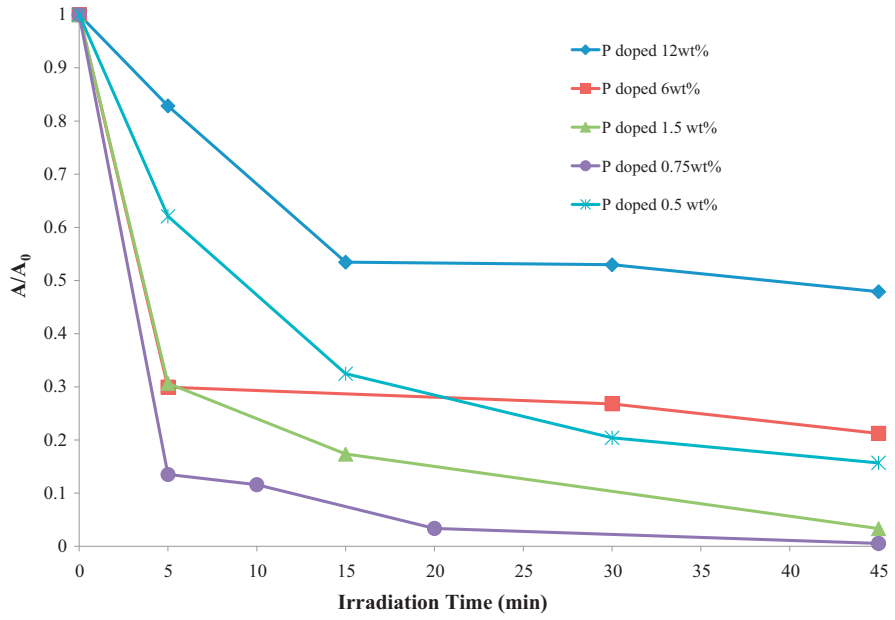

Fig. 7. Effect of phosphorus content on the photocatalytic degradation of rhodamine B irradiated with a 9 W florescent light.

Fig. 7 shows the effect of phosphorus content in TNT on the photocatalytic decomposition of RhB. A reasonable explanation of the optimal P content of 0.75 wt.% is that, as the phosphorus content on the surface of the titania nanotubes increases, the available number of active sites decreases on the photocatalyst surface leading to a decrease in activity (low surface area of 12 wt.% P-TNT, Table 1). The decoloration/degradation of RhB is a complex photocatalytic oxidation process involves deethylation, ring-opening, and mineralization reactions of RhB and intermediates [25–28]. Even so, the oxidative reaction kinetics can be adequately described as a two-phase first-order reaction series by treating intermediates as a group [25]:

$$\text{RhB} \rightarrow \text{intermediateswithchromophoricgroup(s)} \rightarrow \text{leucoproducts} \quad (1)$$

It can be derived according to the Beer–Lambert law and Eq. (1), that the absorbance ratio of A/A_0 at 554 nm is given by:

$$\frac{A}{A_0} = (1-K)\exp(-k_1 t) + K\exp(-k_2 t) \quad (2)$$

and

$$\text{for } t < t_B, \quad \frac{A}{A_0} \cong \exp(-k_1 t) \quad (3)$$

$$\text{for } t > t_B, \quad \frac{A}{A_0} \cong K\exp(-k_2 t) \quad (4)$$

where A_0 and A refer to the absorbance of RhB and intermediates at time 0 and time t; t_B is the break point between Phase I and Phase II degradation of the RhB chromophoric system; k_1 and k_2 are the apparent first-order rate constant for Phases I and II degradation, respectively ($k_1 > k_2$); $K = [k_1/(k_1 - k_2)] \times [\varepsilon_{\text{intermediates}}/\varepsilon_{\text{RhB}}]$, ε_{RhB} is

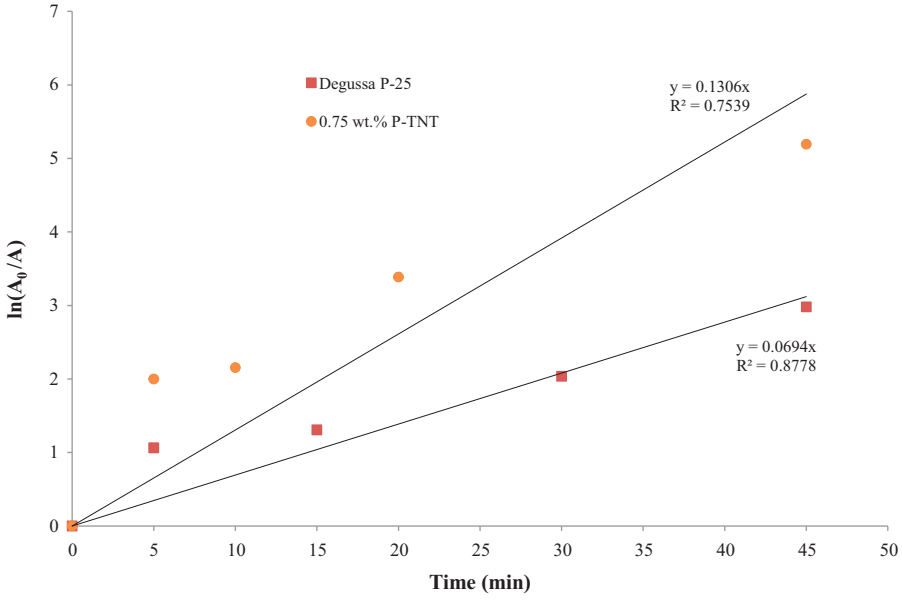

Fig. 8. $\ln(A_0/A)$ vs. time (min) for both 0.75 wt.% P-TNT and Degussa P25 in the degradation of rhodamine B.

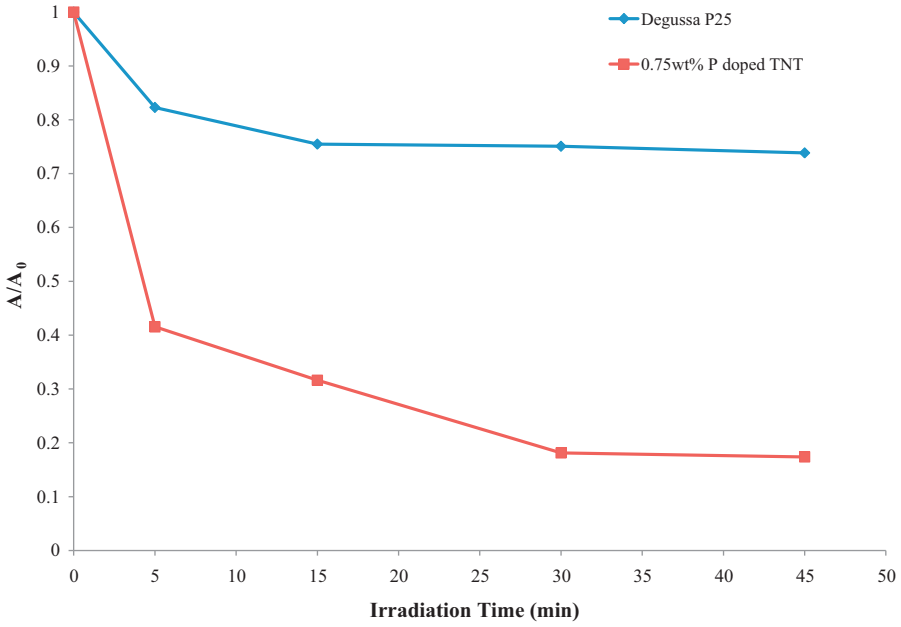

Fig. 9. Degradation of rhodamine B irradiated with a 9 W fluorescent lamp attached with UV filter.

molar absorption coefficient of RhB, and $\varepsilon_{intermediates}$ represents the effective molar absorption coefficient of chromophoric intermediates as a group. In other words, $\ln(A_0/A)$ vs. t has a slope of k_1 in the first phase and a slope of k_2 in the second phase. Due to the 9 W fluorescent light source used and relatively short irradiation time, the observed decolorization is attributed to the fast (Phase I) degradation of the chromophoric system rather than to the slow (Phase II) degradation of chromophoric system of the intermediates. As can be seen in Fig. 8, $\ln(A_0/A)$ vs. time (min) for both 0.75 wt.% P-TNT and Degussa P25 follows the first-order kinetics under the experimental conditions. The results are consistent with literature findings for TiO_2 nanoparticles and other photocatalyst ($Pb_3Nb_4O_{13}$) under similar conditions (albeit under different light sources) [25–28]. The apparent rate constant k_1 is 0.13 min^{-1} for 0.75 wt.% P-TNT and 0.07 min^{-1} for Degussa P25. The apparent rate constants provide a quantitative comparison of photocatalytic activity between 0.75 wt.% P-TNT and Degussa P25. A UV filter (UV Process Supply Inc.), which cuts off the UV light below 385 nm, was attached to the fluorescent lamp and the photoreaction results are shown in Fig. 9. Even though a UV filter is used, Degussa P25 still shows some activity because of the presence of the rutile phase (25%), which is visible light active (up to 410 nm) [29]. Availability of light with wavelengths above 385 nm, which cannot be cut off by the filter may also be responsible for the activity of Degussa P25. For Degussa P25 there is only a 25% decrease in RhB concentration using a UV filter, whereas P-TNT performed well (80% decrease in RhB concentration) because of the visible-light responsive effect induced by doping with phosphorus.

6. Conclusion

Pure titania nanotubes have both monoclinic and anatase phases as seen from XRD analysis. The existence of an $H_2Ti_3O_7$ monoclinic phase is supported by a Ti to O ratio of 3:7, as measured via EDX analysis. TNTs and P-TNTs fabricated through the hydrothermal method all have a high specific surface area compared to Degussa P25 nanoparticles. Doping with phosphorus decreases the surface area but increases the visible-light responsiveness as evidenced by the BET surface analysis and the UV–Vis absorption spectra. For the optimal 0.75 wt.% phosphorus-doping, the surface area decreases from 274 to 272 m^2/g and the band gap decreases from 3.22 eV (TNTs) to 2.95 eV (P-TNTs). Due to phosphorus doping, a discernable shift in the absorption edge towards the visible-light region can be observed, and therefore phosphorus doped titania nanotubes absorb more visible light in the solar spectrum. P-TNTs (0.75 wt.% phosphorus) have the highest activity compared with titania nanoparticles (Degussa P25) and undoped TNTs for the degradation of RhB. The decolorization follows first-order kinetics with the apparent rate constant k_1 of 0.13 min^{-1} for 0.75 wt.% P-TNT and 0.07 min^{-1} for Degussa P25.

Acknowledgements

We thank Mr. Dan Rutman for his kind assistance in EDX measurements, Mr. Sameer Pallavkar for his aid in BET surface area measurements, and Mr. George Spencer for his help in UV–Vis absorption studies.

Appendix A. Supplementary data

Supplementary data associated with this article can be found, in the online version, at doi:10.1016/j.jphotochem.2011.10.001.

References

[1] X. Ye, D. Chen, J. Gossage, K. Li, J. Photochem. Photobiol. A: Chem. 183 (2006) 35–40.
[2] X. Ye, D. Chen, K. Li, V. Shah, M. Kesmez, K. Vajifdar, Chem. Eng. Commun. 194 (2007) 368–381.
[3] D.H. Chen, X. Ye, K. Li, Chem. Eng. Technol. 28 (2005) 95–97.
[4] S. Devahasdin, C. Fan Jr., K. Li, D.H. Chen, J. Photochem. Photobiol. A: Chem. 156 (2003) 161–170.
[5] C.C. Tsai, H. Teng, Chem. Mater. 16 (2004) 4352–4358.
[6] C.A. Grimes, O.K. Varghese, S. Ranjan, Light, Water, Hydrogen: The Solar Production of Hydrogen by Water Photoelectrolysis, first ed., Springer, Norwell, 2007.
[7] H.Y. Niu, J.M. Wang, Y.L. Shi, Y.Q. Cai, F.S. Wei, Micropor. Mesopor. Mater. 122 (2009) 28–35.
[8] H. Li, X. Duan, G. Liu, L. Li, Mater. Res. Bull. 43 (2008) 1971–1981.
[9] J.C. Xu, M. Lu, X.Y. Guo, H.L. Li, J. Mol. Catal. A: Chem. 226 (2005) 123–127.
[10] S. Zhang, Y. Chen, Y. Yu, H. Wu, S. Wang, B. Zhu, W. Huang, S. Wu, J. Nanopart. Res. 10 (2008) 871–875.
[11] L. Deng, S. Wang, D. Liu, B. Zhu, W. Huang, S. Wu, S. Zhang, Catal. Lett. 129 (2009) 513–518.
[12] J. Geng, D. Yang, J. Zhu, D. Chen, Z. Jiang, Mater. Res. Bull. 44 (2009) 146–150.

[13] X. Chen, X. Zhang, Y. Su, L. Lei, Appl. Surf. Sci. 254 (2008) 6693–6696.
[14] H. Sun, Y. Bai, Y. Cheng, W. Jin, N. Xu, Ind. Eng. Chem. Res. 45 (2006) 4971–4976.
[15] D. Gong, C.A. Grimes, O.K. Varghese, W. Hu, R.S. Singh, Z. Chen, E.C. Dickey, J. Mater. Res. 16 (2001) 3331–3334.
[16] A. Ghicov, H. Tsuchiya, J.M. Macak, P. Schmuki, Electrochem. Commun. 7 (2005) 505–509.
[17] J. Qiu, W. Yu, X. Gao, X. Li, Nanotechnology 17 (2006) 4695–4698.
[18] J.H. Lee, I.C. Leu, M.C. Hsu, Y.W. Chung, M.H. Hon, J. Phys. Chem. B 109 (2005) 13056–13059.
[19] T. Kasuga, M. Hiramatsu, A. Hoson, T. Sekino, K. Nihara, Langmuir 14 (1998) 3160–3163.
[20] T. Kasuga, M. Hiramatsu, A. Hoson, T. Sekino, K. Nihara, Adv. Mater. 11 (1999) 1307–1311.
[21] Q. Chen, W.Z. Zhou, G.H. Du, L.M. Peng, Adv. Mater. 14 (2002) 1208–1211.
[22] S. Sakthivel, H. Kisch, Angew. Chem. Int. Ed. 42 (2003) 4908–4911.
[23] H. Znad, Y. Kawase, J. Mol. Catal. A: Chem. 314 (2009) 55–62.
[24] J.C. Yu, J. Yu, W. Ho, Z. Jiang, L. Zhang, Chem. Mater. 14 (2002) 3808–3816.
[25] G. Wei, Y. Zhang, R. Xiong, Chin. Sci. Bull. 48 (2003) 49–52.
[26] M. Makita, A. Harata, Chem. Eng. Process. 47 (2008) 859–863.
[27] O. Merka, V. Yarovyi, D.W. Bahnemann, M. Wark, J. Phys. Chem. C 115 (2011) 8014–8023.
[28] S. Horikoshi, H. Hidaka, N. Serpone, Environ. Sci. Technol. 36 (2002) 1357–1366.
[29] D.C. Hurum, K.A. Gray, T. Rajh, M.C. Thurnauer, J. Phys. Chem. B 108 (2004) 16483–16487.